XLIII CILAMCE
21–25, November, 2022
FOZ DO IGUAÇU – PR – BRAZIL

Sensitivity and Aerodynamic Analysis of a Darrieus Wind Turbine Using Different Geometric Parameters

Pedro Henrique B. B. Martinez[1], Leandro O. Salviano[1]

[1]*Dept. of Mechanical Engineering, São Paulo State University*
Ilha Solteira, 15385-000, SP, Brazil
p.barros@unesp.br, leandro.salviano@unesp.br

Abstract. Considering the demand for renewable energy, this work has the objective of contributing to the development of Small-Scale Darrieus Vertical Axis Wind Turbine that can be employed in decentralized electrical generation through computational fluid dynamics, operating at a low tip speed ratio (TSR). A 2D numerical modeling is performed with unsteady-state and turbulent flow. Geometric parameters analyzed are profile camber (m), camber position (p), profile thickness (t), chord (c) and pitch angle (β), the first three being based on NACA-4 digit parameterization. A sensitivity analysis using the Smoothing Spline ANOVA algorithm is conducted to predict the influence of each parameter on the power coefficient ($\overline{C_p}$) of the turbine. Two Designs of Experiments (DoE) were created with 100 and 192 possible configurations of the Darrieus turbine, so it was possible to evaluate which parameters and interaction of them have the most influence on $\overline{C_p}$. The main finds showed that the pitch angle (β) contribution on $\overline{C_p}$ is the highest among others (69%). An analysis considering only the geometry of the blades profile showed its influence on the flow through the turbine. Finally, an increase in aerodynamic efficiency of Darrieus VAWT is the main responsible for increasing $\overline{C_p}$.

Keywords: Darrieus turbine, Sensitivity analysis, Aerodynamic efficiency, NACA-4 digit.

1 Introduction

Following the population and economic growth tendencies, it is believed that the demand for primary and renewable energy sources will increase rapidly in the near future, even if there are efforts to improve the efficiency of energy consumption (Kc *et. al.* [1]). Fossil fuels still account for the largest share of energy generation worldwide: for example, in 2018, natural gas, oil and coal accounted approximately 80% of global final energy consumption according to British Petroleum [2]. On the other hand, stricter environmental regulations, the depletion of fossil fuel reserves and environmental warming threats have aroused interest in the development of alternative sources for energy generation, it is in this context that renewable energy sources like wind energy are necessary to guarantee sustainability and preservation of the environment.

Wind power generation has the lowest relative emission of greenhouse gases and the lowest water consumption according to Evans *et. al.* [3]; in addition, wind power generation is considered the most economical among the different renewable alternatives as stated by Ghasemian *et. al.* [4]. Considering such information, the global accumulated installed capacity of wind energy has been increasing substantially year after year, notably in China, the United States, Europe, India and Brazil. Although in recent times much of the progress in wind energy has been due to the installation of large-scale wind farms both onshore and offshore, it is unclear whether such large-scale wind farms are indeed a sustainable approach to wind farms. Several studies have already addressed the concern about spreading wind farm over large areas of land or water in such a way that it can impact local- or even global – climatic conditions, as showed for example by Fiedler and Bukovsky [5] and Wang and Prinn [6].

A potential solution for capturing wind energy that has emerged is the decentralized use of small-scale wind turbines, especially in the built environment and in off-grid locations. Van Hooff *et. al* [7] said that small-scale wind turbines with a output power of around 10 kW are sufficient for domestic needs. Another benefit is that power generation within cities an off-site locations can represent a great step towards reducing both the grid

generation load and the power transmission infrastructure (Ishugah [8]).

This work proposal considers a Vertical Axis Wind Turbine (VAWT) of Darrieus type used for decentralized energy generation. A 2D numerical modeling is performed considering the assumptions of unsteady-state and turbulent flow in order to perform Computational Fluid Dynamics (CFD) simulations. Using the Grid Convergence Index (GCI) methodology mesh sensitivity analysis is ensured. The numerical robustness is verified through experimental comparison. This work analyzes the following geometric parameters of the VAWT: profile camber (m), camber position (p), aerodynamic profile thickness (t), profile chord (c) and pitch angle (β), the first three being based on NACA-4 digit parameterization. Associated with the operational parameters, these geometric parameters are submitted to a sensitivity analysis using the Smoothing Spline ANOVA algorithm in order to predict the influence of each one of these on the power coefficient ($\overline{C_p}$).

2 Methodology

For this work 2D simulations was carried out for a 3-bladed VAWT with NACA-4 digit airfoils, diameter (D) equal to 1.03m at constant tip speed ratio (TSR) λ=2.63 (see Fig. 1). The 2D simulation represents the midplane of a turbine with high aspect ratio where the 3D tip effects are small according to Rezaeiha [9].

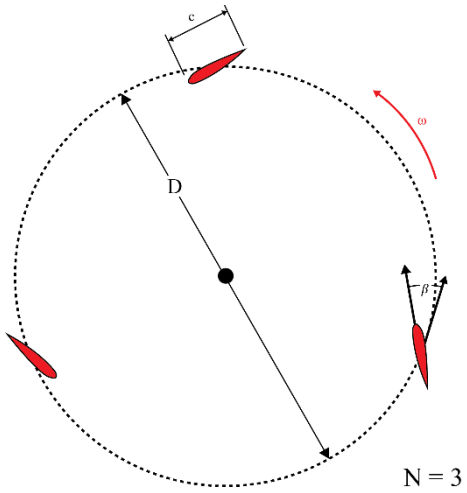

Figure 1. Representation of a 3-bladed Darrieus VAWT highlighting the number of blades (N), rotor diameter (D), chord length (c) and pitch angle (β)

Namely, the five geometric parameters considered for the sensitivity analysis in this research are the profile camber (m), camber position (p), aerodynamic profile thickness (t) (see Fig. 3) and pitch angle (β), the first three being based on the NACA-4 digit parameterization.

2.1 Aerodynamics of Darrieus wind turbines

According to Rezaeiha [10] the complexity of Darrieus turbines is commonly attributed to unstable power conversion due to large variations of the angle of attack (α) and the effective velocity captured by the blades during each revolution. An azimuthally dependent effective velocity U_{eff} is experienced by the blades as function of the freestream velocity (U_∞) and the turbine rotation expressed in terms of its tangential and normal components, as

showed by Trentin *et. al.* [11] and represented on Fig. 2.

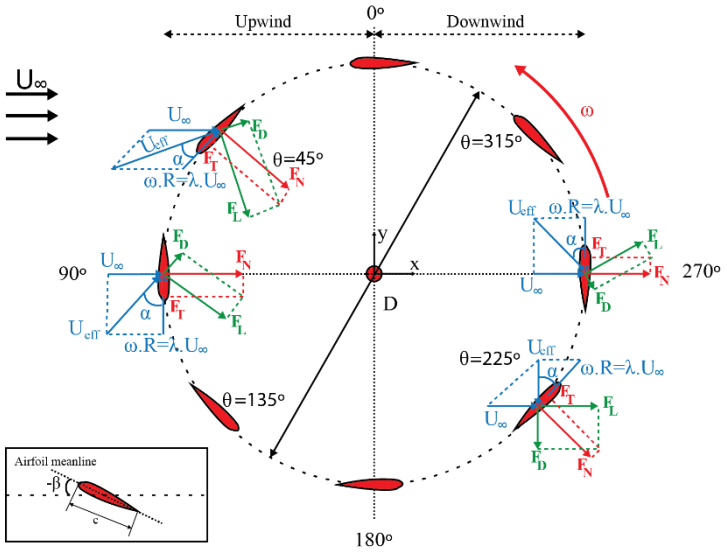

Figure 2. Schematic representation of aerodynamic forces, velocities, and angle of attack (α) at different azimuthal positions

The tangential and normal components of U_∞ are expressed in eq. (1) - eq.(3).

$$U_T = \omega_r R - U_\infty sin\theta \tag{1}$$

$$U_N = U_\infty cos\theta \tag{2}$$

$$U_{eff} = \sqrt{U_T^2 + U_N^2} \tag{3}$$

Drag force (F_D) and lift force (F_L) are generated by the airflow over the blades of Darrieus VAWT. Both forces are expressed into their normal and tangential components on eq. (5) – eq. (6).

$$F_N = F_L cos\alpha + F_D sin\alpha \tag{4}$$

$$F_T = F_L sin\alpha + F_D cos\alpha \tag{5}$$

Therefore, lift coefficient (C_l) and drag coefficient (C_d) can be expressed as:

$$C_l = \frac{F_L}{\frac{1}{2}\rho U_\infty^2 A} \tag{6}$$

$$C_d = \frac{F_D}{\frac{1}{2}\rho U_\infty^2 A} \tag{7}$$

Lastly, the power coefficient (C_p) can be computed by multiplying the torque coefficient (C_t) and TSR (λ).

$$C_t = \frac{T}{\frac{1}{2}\rho A R U_\infty^2} \tag{8}$$

$$\lambda = \frac{\omega_r R}{U_\infty} \tag{9}$$

$$C_p = \lambda C_t \tag{10}$$

2.2 NACA-4 digit parameterization

The airfoil geometric parameters are obtained by NACA-4 digit parameterization. This one makes a systematic representation of airfoils based on the thickness (t), profile camber (m) and its respective position (p) as shown in Fig. 3, stated and demonstrated by Barros and Salviano [12].

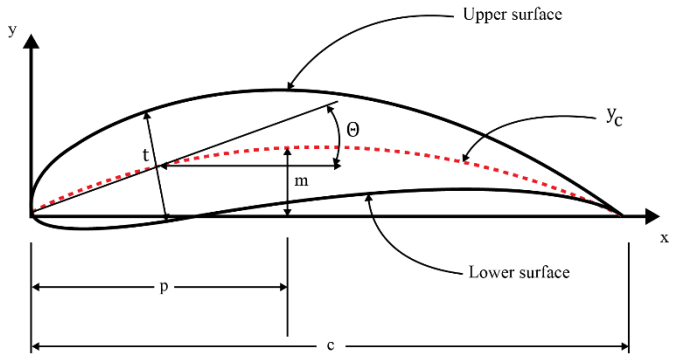

Figure 3. NACA-4 digit airfoil

2.3 Governing equations

Flow dynamics through the Darrieus VAWT was modeled using the Unsteady Reynolds-Averaged Navier-Stokes (URANS) approach using the Coupled algorithm for the pressure-velocity coupling as suggested by Rezaeiha [10], and Hashem and Mohamed [13]. The discretization was performed using the Finite Volume Method (FVM), considering the assumptions of 2D, incompressible, turbulent, and unsteady flow as performed by Trentin *et. al.*[11], Barros and Salviano [12] and Bai [14].

Considering the assumptions described, the continuity and momentum equations can be expressed, respectively as:

$$\frac{\partial u_i}{\partial t} + \frac{\partial u_i}{\partial x_i} = 0 \tag{11}$$

$$\frac{\partial u_i}{\partial t} + u_i \frac{\partial u_i}{\partial x_j} = -\frac{1}{\rho}\frac{\partial p}{\partial x_i} - \frac{\partial}{\partial x_j}\left[\nu\left(\frac{\partial u_i}{\partial x_j} + \frac{\partial u_j}{\partial x_i} - \frac{2}{3}\delta_{ij}\frac{\partial u_i}{\partial x_i}\right)\right] + \frac{\partial}{\partial x_j}\left(-\overline{u_i' u_j'}\right) \tag{12}$$

The Reynolds stress tensor was modeled in terms of mean flow parameters adopting the four-equation turbulence model Transition SST (Shear Stress Transport), one of the Rezaeiha [10] suggestions. In addition, compared with the SST k-ω model, the Transition SST model requires less revolutions to achieve a stable solution and converges faster within each temporal loop as was found by Trentin *et. al.* [11]. Both momentum and turbulence equations have been discretized using second order schemes.

2.4 Computational domain and boundary conditions

In addition to what was previously presented, this work investigates a small-scale Darrieus VAWT operating under a freestream velocity (U_∞) of 9 m/s keeping a constant λ=2.63. In order to numerically model the turbine rotation, the computational domain was subdivided into two subdomains: a stationary domain and a rotating core in which the turbine is located. In this rotating core was also adopted a small circular region close to the blades, used only to control the mesh quality. So, a sliding interface between the stationary domain and the rotating core allows the turbine rotation, as shown in Fig. 4.

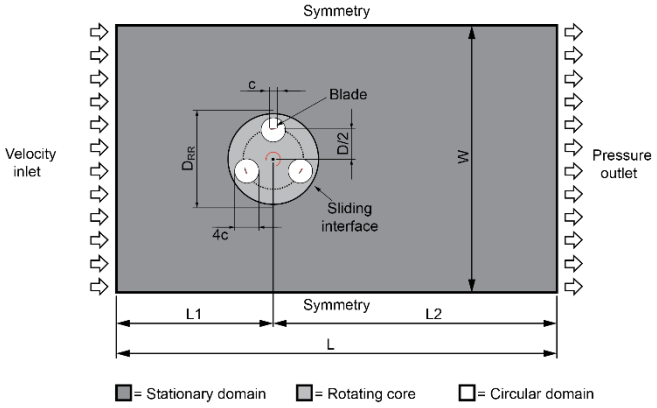

Figure 4. Schematic representation of the computational domain and boundary conditions adopted

All dimensions of the computational domain were defined based on well-established recommendations presented previously and summarized in Tab. 1

Table 1. Computational domain dimensions

Parameter	Nomenclature	Value
Inlet Distance	L_1	10D
Outlet Distance	L_2	15D
Rotating Domain Diameter	D_{RR}	1.5D
Domain Width	W	20D

Regarding to boundary conditions were adopted uniform velocity and a 5% turbulence intensity at the inlet, constant gauge pressure at outlet, symmetry at top and bottom faces, no-slip at blade walls and sliding at the interface between the domains. In order to achieve the stability of the adjective flux through the interface, equally sized cells were generated at both sides of the sliding interface.

Looking to a well known suggested criterion of $y^+ \approx 1$, the size of the first element on the blade profile was defined. In addition, this criterion is also necessary for the Transition SST turbulence model. Particularly, 22 layers with a growth rate of 1.2 and total thickness of 0.004 m were created, so the maximum y^+ achieved was 0.87. The mesh quality was finally evaluated based on non-orthogonality and skewness criteria which the maximum values were 75° and 0.96, respectively. The computational mesh is shown in Fig. 5.

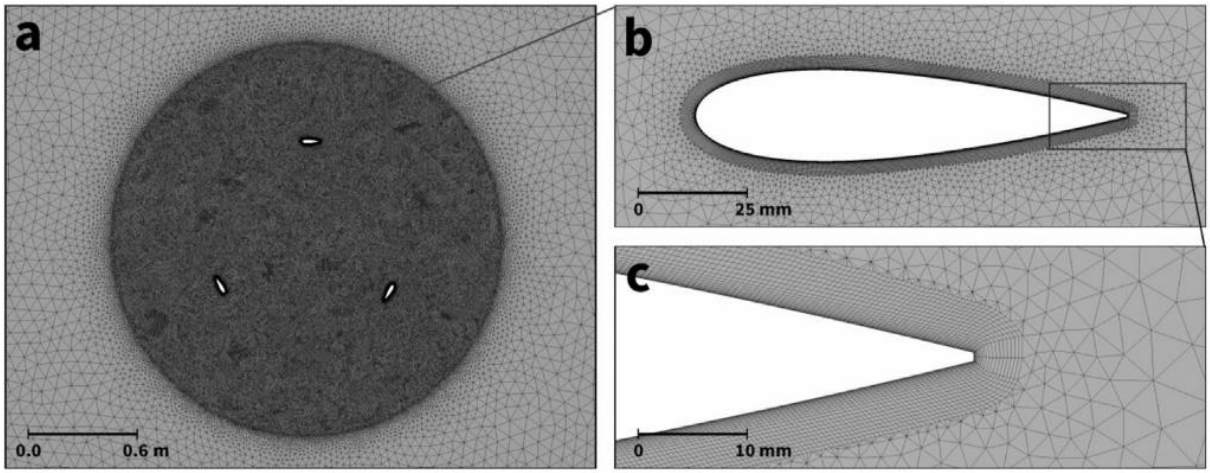

Figure 5. Computational mesh: (a) interface between stationary and rotating domains; (b) refined mesh around the airfoil; (c) layers of prismatic elements on the airfoil

2.5 Grid convergence analysis and numerical settings

A grid independence study was performed based on GCI methodology formulated by Celik *et. al.* [15] to quantify mesh discretization errors, this is a well-established practice in CFD according Tummalla *et. al.* [16] and Balduzzi *et. al.* [17] for example. For that, were considered three mesh configurations with 152,118 (coarse), 262,123 (medium) and 450,947 (refined) cells in the rotating core, resulting in a refinement ratio of approximately 1.3 as suggested by the methodology. In the stationary domain the number of cells was kept constant, with approximately 240,000. All the mesh characteristics on the blades were also kept constant, i.e., number of layers on the blade, growth ratio and total thickness.

The reference case for both GCI methodology and the validation with experimental data also summarizing the main simulation settings described previously is indicated in Tab. 2.

Table 2. Main features and main simulation settings of validation model

Parameter	Nomenclature	Value
Aerodynamic profile	NACA 0021	
Profile chord	c	0.0858 m
Turbine rotor diameter	D	1.03 m
Number of blades	N	3
Mesh Type	Unstructured triangular	
Freestream Velocity	U_∞	9 m/s
Outlet Pressure	P	1 atm
Angular step	$\Delta\theta$	0.5°
Pitch Angle	β	0°
Tip Speed Ratio	λ	2.63
Turbulence Model	Transition SST	
Solver	Pressure-based	
Fluid properties	Incompressible	
Pressure-velocity solution algorithm	Coupled	
Iterations per angular step		30
Maximum residuals per angular step		10^{-4}
Revolutions for convergence/data extraction		10

This reference case is based on the work developed by Castelli *et. al.* [18].

The results of GCI analysis are showed in Tab. 3 in which the numerical uncertainty in the solution between the two most refined meshes is about 0.27%. This small percentage of uncertainty justifies the choice of using the medium mesh instead the refined one for the simulations.

Table 3. Results of GCI considering three meshes. Number of cells represents the number in the rotating core

Parameter	Nomenclature	Value
Fine mesh	Number of cells	450,947 elements
Medium mesh	Number of cells	262,123 elements
Coarse mesh	Number of cells	152,118 elements
Maximum y^+ for fine mesh	y_1^+	0.39
Maximum y^+ for medium mesh	y_2^+	0.87
Maximum y^+ for coarse mesh	y_3^+	34.9
Power Coefficient for fine mesh	$\overline{C_{p_1}}$	0.303
Power Coefficient for medium mesh	$\overline{C_{p_2}}$	0.294
Power Coefficient for coarse mesh	$\overline{C_{p_3}}$	0.184
Grid Convergence Index	GCI_{21}	0.268%

Additionally to increasing the confidence on the numerical model, the GCI analysis assists in selecting an adequate mesh size without overshooting, which would considerably increase the processing time per simulation on the sensitivity analysis.

2.6 Angular step analysis

In order to analyze the influence of the angular step on the power coefficient, were performed a comparative analysis considering three angular steps using the same characteristics of the validation model summarized in Tab. 2 and described with more details in chapter 3. Table 4 shows this comparative analysis for 1.0°, 0.5° and 0.25°.

Table 4. Difference in the power coefficient ($\overline{C_p}$) between the experimental data and the numerical results

Parameter	Nomenclature	Value	Value	Value
Angular step	$\Delta\theta$	1.0°	0.5°	0.25°
Percentage difference in $\overline{C_p}$		8.01%	5.45%	2.88%

The literature indicates that the angular step should be as small as possible for a better representation of the physical phenomena, but as presented by Trentin *et. al.* [11], although an angular step of 0.25° provides the closest results to the experimental data found by Castelli *et. al.* [18], the computational resource required for the proposed analysis would be tremendous once a single case running on eight high performance computing nodes (total of 64 CPU cores) can take up to 30 wall-clock hours to complete 10 revolutions. Therefore, considering the trade-off between accuracy and processing time, the choice of an angular step of 0.5° seemed reasonable, as it requires less computational effort to run the sensitivity analysis, while ensuring good physical reliability. For $\Delta\theta$=1.0°, as discussed by Balduzzi *et. al.* [17] and demonstrated by Trentin *et. al.* [11], the Courant-Friedrichs-Lewy (CFL) criterion is not met at the sliding interface, which may lead to incorrect predictions for adjective flux through the interface causing a discrepancy on numerical results. An angular step of 0.5° was also successfully used by Bai *et. al.* [14] and Li *et. al.* [19].

3 Numerical validation

For the numerical validation, the results of this work numerical model were compared with experimental data obtained from measurements in a wind tunnel by Castelli *et. al.* [18], considering the same geometric and operational parameters previously showed in Tab. 2. In addition, the results were also compared with numerical validations published by Rezaeiha [10] and,Hashem and Mohamed [13] which validated their numerical model against the same experimental data used here. This approach is summarized in Fig.6.

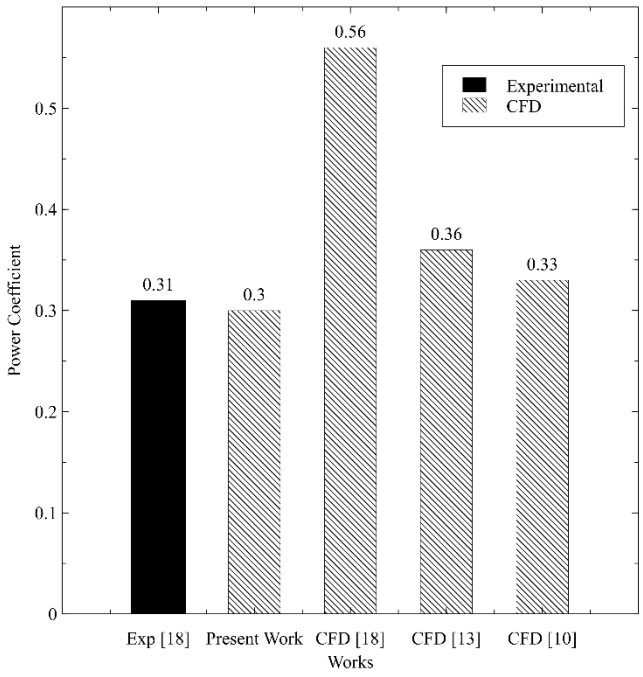

Figure 6. Comparison between experimental data and numerical validation results

From Fig. 6 is possible to see that the power coefficient ($\overline{C_p}$) resulting from this present numerical modeling closely agrees with the experimental data from Castelli *et. al.* [18], i.e., is able to adequately reproduce the aerodynamic behavior of small-scale Darrieus VAWT with similar characteristics.

The large difference between CFD and experimental results presented by Castelli *et. al.* [18] is probably, among other considerations, the use of $\Delta\theta$=1.0°, thus the Courant-Friedrichs-Lewy (CFL) criterion is not met at the sliding interface, which may lead to incorrect predictions for adjective flux through the interface causing a discrepancy on numerical results, as already discussed before.

3.1 Sensitivity analysis using Smoothing Spline-ANOVA methodology

A promising approach for extracting information from numerous and noisy data according Helwig and Ma [20]

is the Smoothing Spline-ANOVA (SSANOVA) methodology. Using this methodology is possible to model multivariate data and provide nice interpretability of modeling and prediction outcome as described by Gu [21]. In addition SSANOVA models have been shown to have desirable asymptotic properties as observed by Gu [21], Li [22] and Wahba [23].

The advantage of SSANOVA method is the visualization of some relationships between the input variables (parameters), which is not easily observed when parametric regression methods are used, according to Ricco and Turco [24]. However, this statistical method usually requires high computational resources, which is a function of both the complexity of the problem and the size of the sample, which happens in this work. The SSANOVA method represents a suitable screening technique to detect important variables (parameters) in a dataset.

3.2 Design of Experiments (DoE)

Design of Experiments is defined as a branch of applied statistics that deals with the planning, condution, analysis and interpretation of controlled tests to assess the factors that control the value of a parameter or group of parameters according to Wang [25]. In summary, the DoE provides a distribution of the input variables in a sample field, thus allowing the application of statistical tools to identify the main effects and interaction between the variables (parameters).

One of the several approaches to determine the set of design points (unique combinations of independent variables settings) to be used in DoE is the Uniform Latin Hypercube Sampling (ULHS).

In this work is used ULHS to create an initial DoE containing 100 possible configurations and after a bigger DoE containing 192 possible configurations of the Darrieus VAWT, considering the parameters to be analyzed and their respective operational range shown in Tab. 5.

Table 5. Parameters for making the DoE

Parameter	Nomenclature	Operational range	Increment
Profile camber	m	0 - 9	1
Camber position	p	1 - 9	1
Profile thickness	t	5 - 40	1
Profile chord [m]	c	0,05 - 0,20	0.5
Pitch angle [°]	β	-15 - 15	0.1

4 Results

The entire DoE containing 100 possible configurations of Darrieus VAWT and the second one containing 192 was simulated using the same boundary and operational conditions (see Tab. 2) to evaluate which parameters and

interactions of them have the most influence on the power coefficient. Some of the results of both DoEs are shown

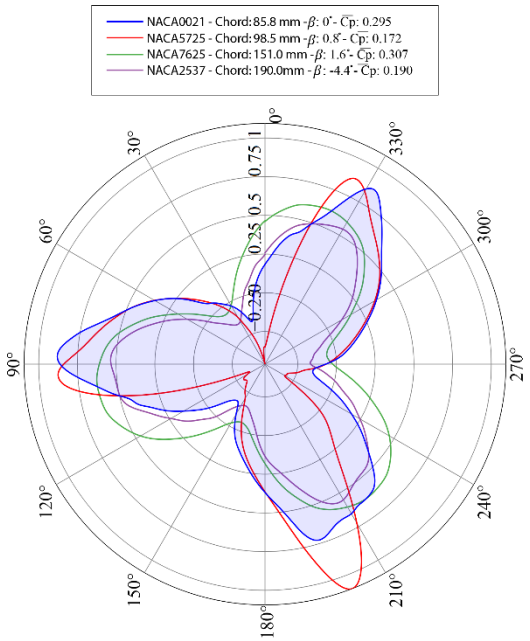

in Fig. 7.

Figure 7. Comparison of instantaneous C_p and $\overline{C_p}$ for some configurations of Darrieus VAWT

With both DoE containing 100 and DoE containing 192 Darrieus VAWT configurations and the results of the simulation of each one it was possible to submit them to a sensitivity analysis using SSANOVA in order to predict the influence of the parameters (input variables) described in Tab. 5 on the power coefficient ($\overline{C_p}$). Figure 8 shows the ranking of input variables interaction effects on $\overline{C_p}$ for both DoEs.

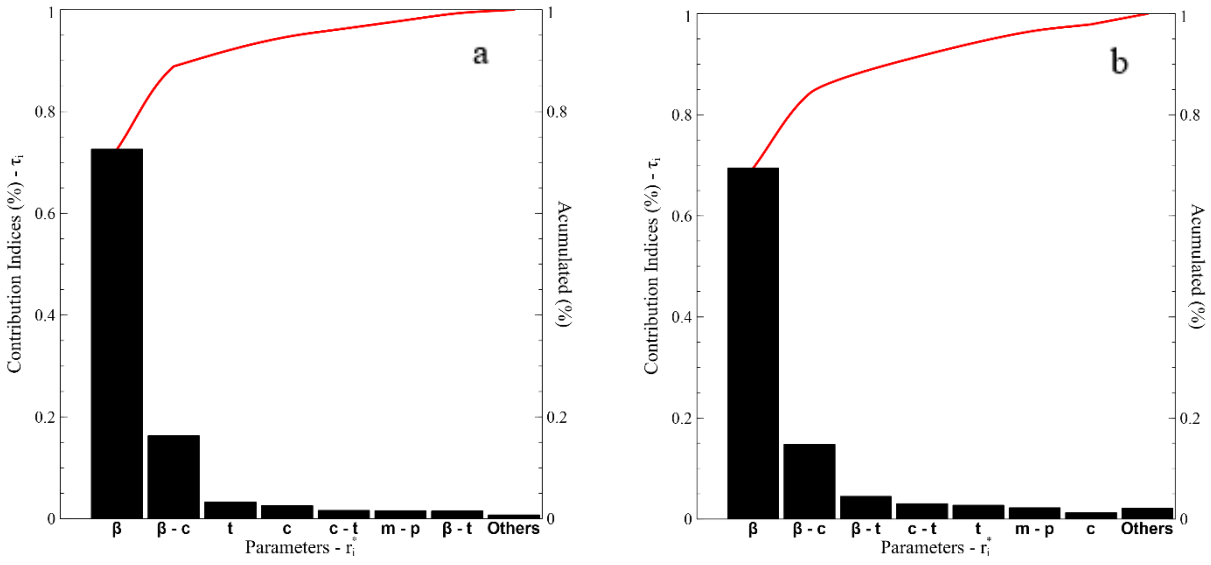

Figure 8. Ranking of the main and interaction effects of the input variables on $\overline{C_p}$: for DoE containing 100 (a) and containing 192 configurations (b).

The main finds showed that the contribution of pitch angle (β) on the power coefficient ($\overline{C_p}$) was the highest among the others, with a contribution of 73% considering DoE containing 100 and 69% considering a bigger DoE with 192 configurations. Another significant contribution is the combination of pitch angle (β) and the profile chord (c), presenting an index of 16% and 15% considering the DoE with 100 and 192, respectively. Therefore, the impact of NACA 4-digit parameterization on $\overline{C_p}$ is relatively small. Morevover, the sum of the contribution of the parameters inherent to the parameterization is only 4% and 6% considering the DoE with 100 and 192,

respectively. In general, it can be said that there is a certain agreement of values between the two DoEs.

Trying to demonstrate the effect of β on $\overline{C_p}$, simulations for the same NACA airfoil with the same chord (c) and with only different values of β were carried out. Figure 9 shows the results of simulations.

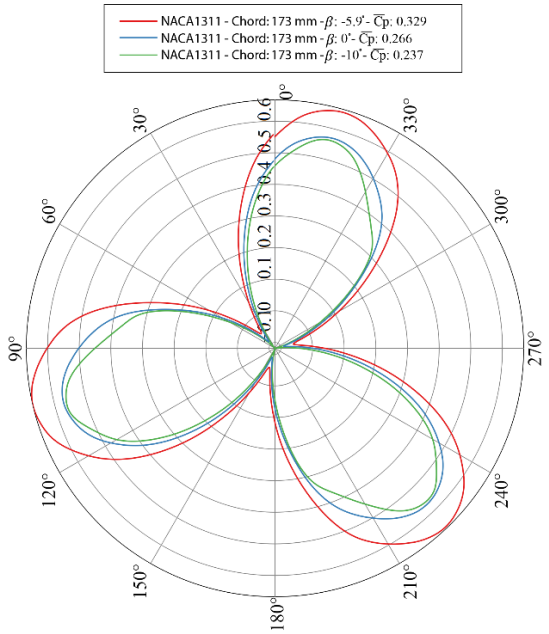

Figure 9. Comparison of instantaneous C_p and $\overline{C_p}$ for NACA 1311 with c = 173mm and different β

It can be seen in Fig. 9 that the decrease in pitch angle to a certain point tends to increase $\overline{C_p}$, but after a certain point it can mean a decrease in $\overline{C_p}$. Another effect perceived on both DoEs and already stated by Rezaeiha *et. al.* [9] and also observed by Trentin *et. al.* [11] was that the positive pitch angles tend to influence the power coefficient more than their positive counterpart (positive values of β tend to decrease significantly $\overline{C_p}$). A better understanding comes from analyzing the mechanisms driving and dragging the turbine motion, like lift and drag coefficients.

It is necessary to point out that for each profile defined by NACA-4 digit parameterization, the pitch angle that allows greater and lesser aerodynamic efficiency is different, since this parameterization allows the creation of different symmetrical and asymmetrical profiles. In all cases, the pitch angle directly influences the flow around each profile and also the flow during the turbine rotation causing an interaction effect between the blades.

Although the influence of the geometric parameters of the NACA-4 digit parameterization on $\overline{C_p}$ is small (4% for the first DoE), is not possible to say that they are irrelevant, after all many aspects of the physical phenomenon are associated with the geometry of the airfoil. Therefore, a better detailing of the impacts of theses aerodynamic aspects on the wind turbine conversion performance is of this work interest. Thus, initially, the pitch angle (β) was removed in the analysis (fixing β) considering the sample with 100 configurations. This approach resulted in inadequate collinearity indices (far from 1 as needed from the SSANOVA) to ensure the robustness of the SSANOVA method. It is at this point that the limitation of the first DoE is revealed and the need to add more configurations (92) and generate a large sample totaling 192 configurations (second DoE). This DoE containing 192 configurations reach collinearity indices very close to 1 (approximately 1.04) when considering the pitch angle remotion for sensitivity analysis. Performing the SSANOVA method but considering only the geometric parameters (fixed β) of the airfoil, it is possible to analyze the contribution of each one of them on $\overline{C_p}$. The results of this new analysis are shown in Fig. 10.

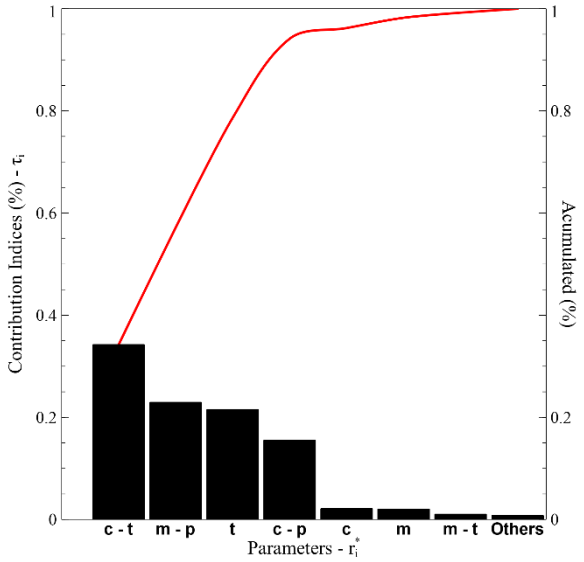

Figure 10. Ranking of main and interaction effects of airfoil geometric parameters (fixed β) on $\overline{C_p}$

As showed in Fig. 10 the combination of the chord (c) and thickness of airfoil (t) have a contribution of 34% on $\overline{C_p}$, also is possible to see that among the most significant indices is found the combination of the maximum camber (m) and camber position (p) presenting 23% and, a main effect contribution of profile thickness (t) with 21% on $\overline{C_p}$. According to this new analysis, it is possible to show that the NACA-4 digit parameterization is not irrelevant to the performance of a Darrieus VAWT, which could be hastily said looking only at the sensitivity analysis that considered the pitch angle (β) variation (Fig. 8).

Finally, with all 192 configurations, the one with the highest $\overline{C_p}$ is composed by the following parameter values: NACA 6427 (m=6, p=4, t=27), c=137mm and β=0°. This specific configuration presented a $\overline{C_p}$=0.35, as shown in Fig. 11 in comparison with the validation (base) model.

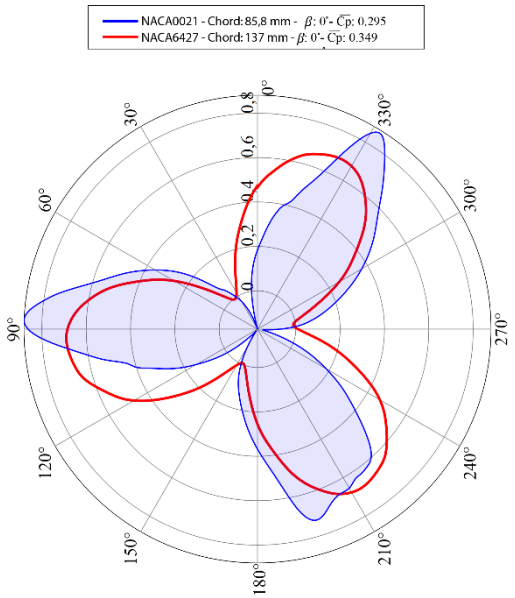

Figure 11. Comparison of instantaneous C_p and $\overline{C_p}$ between the configuration with highest $\overline{C_p}$ and base model

The influence of the pitch angle on $\overline{C_p}$ of this Darrieus VAWT configuration with NACA 6427 and c=137mm is shown in Fig. 12.

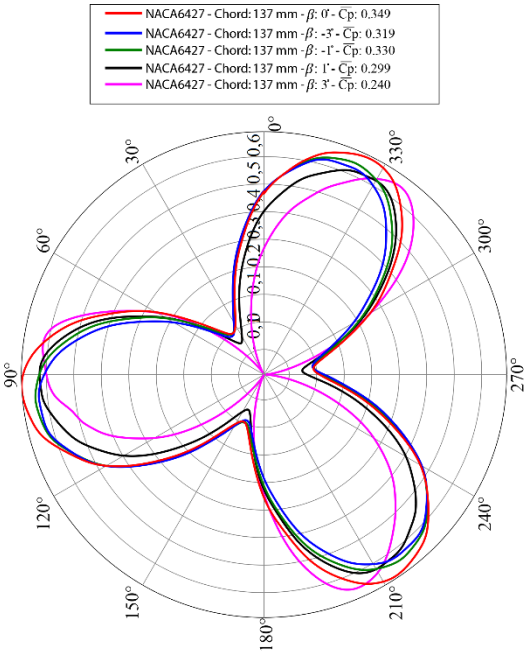

Figure 12. Comparison of instantaneous C_p and $\overline{C_p}$ for NACA 6427 with c=137mm and different β

It is possible to identify the influence of the flow behavior through the turbine blades on $\overline{C_p}$ by surveying the aerodynamic coefficients $\overline{C_l}$, $\overline{C_d}$ and the aerodynamic efficiency $\overline{C_l}/\overline{C_d}$. Considering all sample, it was possible observing that an increase in lift ($\overline{C_l}$) should be accompanied by a low drag ($\overline{C_d}$), causing an increase on aerodynamic efficiency ($\overline{C_l}/\overline{C_d}$) in order to achieve high power coefficient ($\overline{C_p}$).

This observed aerodynamic aspects are summarized for different configuration of Darrieus VAWT on Fig 13.

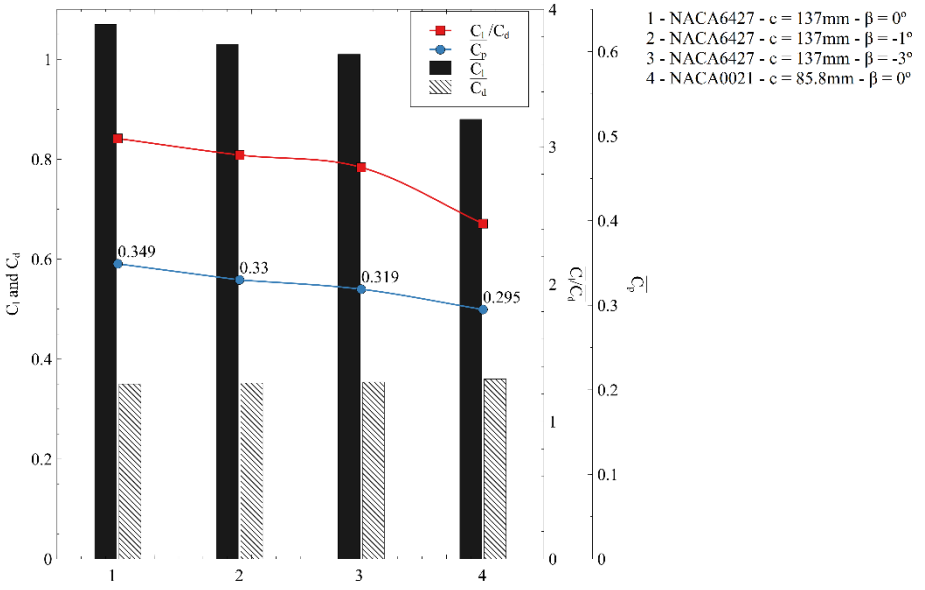

Figure 13. Comparison of $\overline{C_p}$ using $\overline{C_l}$ and $\overline{C_d}$ for different Darrieus VAWT configurations

Although configurations 1 and 4 of Fig. 13 have the same pitch angle ($\beta = 0°$), the change in the chord (c) and in the parameters of the NACA-4 digits profile also reflects on the aerodynamic behavior of the Darrieus VAWT.

For a broader view of the physical aerodynamic phenomena due to the flow though the Darrieus VAWT, velocity fields of the maximum and minimum instantaneous C_p points (θ positions) are shown in Fig. 14 and in

Fig.15 for configuration 1 and 4 from Fig. 13, respectively.

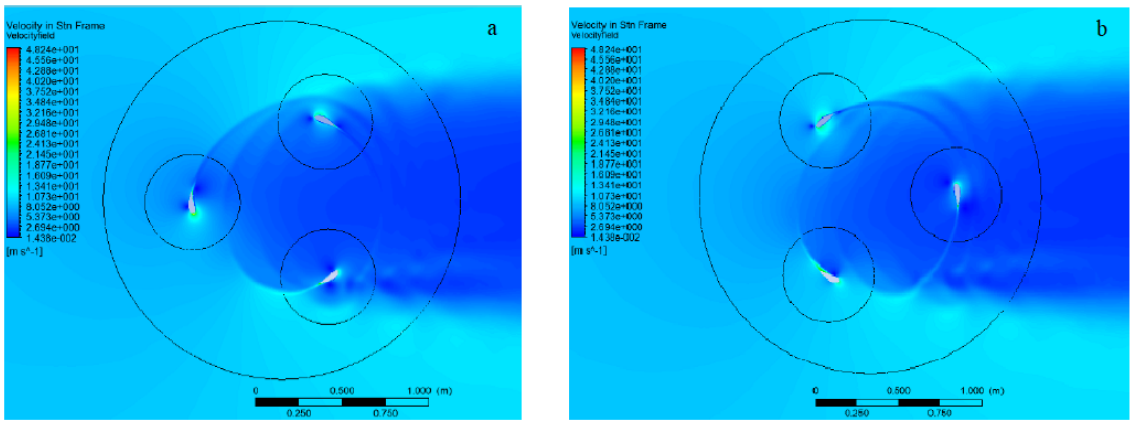

Figure 14. Velocity field of Darrieus VAWT with NACA6427 with c=137mm and β=0°. a) Minimum $C_p$at θ=95º and (b) maximum C_p at θ=155°

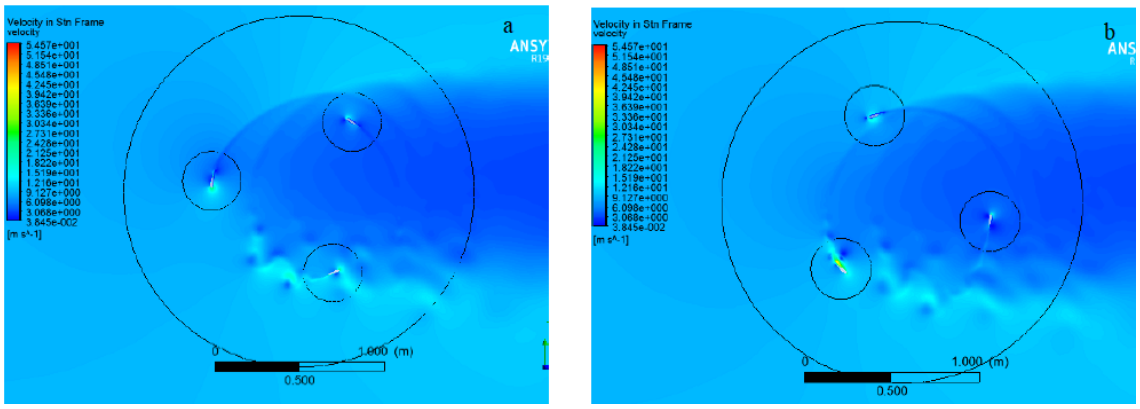

Figure 15. Velocity field of Darrieus VAWT with NACA0021 with c=85.8mm and β=0°. a) Minimum $C_p$at θ=88º and (b) maximum C_p at θ=143°

Analyzing Fig. 14 and Fig. 15 it is possible to notice that at the points of maximum and minimum $\overline{C_p}$ the flow is more unstable for configuration 4 (validation model) than in the configuration with the highest $\overline{C_p}$ of the sample. This unstable flow reduces the average aerodynamic efficiency $\overline{C_l}/\overline{C_d}$ of the turbine and consequently the value of $\overline{C_p}$. Thus, it stated that the increase in lift forces associated with low drag forces caused an increase on $\overline{C_p}$.

5 Conclusions

The sensitivity analysis using the SSANOVA method in order to predict the influence of geometric input parameters of Darrieus VAWT on the power coefficient ($\overline{C_p}$), using 2D numerical simulations considering unsteady-state and turbulent flow for all 192 possible configurations showed that the contribution of pitch angle (β) on the power coefficient was the highest among the other parameters, with a contribution of 69%. Another significant contribution is the conbination of pitch angle (β) and the profile chord (c), presenting an index of 15%.

Although the influence of the geometric parameters from the NACA-4 digit parameterization on $\overline{C_p}$ is small (4% for DoE containing 100 and 6% for DoE with 192 configurations), it is not possible to say that they are irrelevant, after all, many aspects of the physical phenomenon are associated with the geometry of the aerodynamic profile blades, as demonstrated in the analysis conducted with fixed β for DoE with 192 configurations. This second analysis showed that considering solely the airfoil geometry parameters ,the combination of the chord (c) and thickness of airfoil (t) have a contribution of 34% on $\overline{C_p}$ of Darrieus VAWT, also is possible to see that among the most significant indices is found the combination of the maximum camber (m) and camber position (p) presenting 23% and, a main effect contribution of profile thickness (t) with 21% on $\overline{C_p}$.

Through the study of the aerodynamic study of the turbines, it was concluded that the increase in lift coefficient ($\overline{C_l}$), associated with low drag coefficient ($\overline{C_d}$) so the aerodynamic efficiency ($\overline{C_l}/\overline{C_d}$) is large as possible, causes

an increase on $\overline{C_p}$.

Finally, among allthe sample configurations, we can highlight that the turbine that presented the highest $\overline{C_p}$ has the following set of parameters: NACA6427 blades profile, chord (c)=137mm and pitch angle (β)=0°. This configuration presented a $\overline{C_p}$=0.349, that is 18,3% larger that the base model $\overline{C_p}$ (0.295).

The results of this work are valid only for TSR=2.63, extrapolations to other TSR values should be investigated, since no analyzes were made for such cases.

Authorship statement. The authors hereby confirm that they are the sole liable persons responsible for the authorship of this work, and that all material that has been herein included as part of the present paper is either the property (and authorship) of the authors.

References

[1] A. Kc, J. Whale and T. Urmee, "Urban wind conditions and small wind turbines in the built environment: A review". Renewable Energy, vol. 131, 2019.
[2] British Petroleum, "BP Statistical Review of World Energy Report". London, UK.
[3] A. Evans, V. Strezov and T. J. Evans, "assessment of Sustainability Indicators for Renewable Energy Technologies". Renewable and Sustainable Energy Reviews, vol.13, 2009.
[4] M. Ghasemian, Z. N. Ashrafi and A. Sedaghat, "A review on computational fluid dynamic simulation techniques for Darrieus vertical axis wind turbines". Energy Conversion and Management, vol. 149, 2017.
[5] B. H. Fiedler and M. S. Bukovsky, "The effect of a Giant Wind Farm on Precipitation in a Regional Climate Model". Environmental Research Letters, vol.6.
[6] C. Wang, R. G. Prinn, "Potential Climatic Impact and Reliability of Very Large-Scale Wind Farms", Atmospheric Chemistry and Physics, vol. 10, 2010.
[7] T. Van Hoof *et. al.*, "A venturi-shaped roof for wind-induced natural ventilation of buildings: Wind tunnel and CFD evaluation of different design configurations". Building and Environment, vol. 46, 2011.
[8] T. Ishugah, Y. Li, R. Wang and J. Kiplagat, "Advances in Wind Energy Resource Exploitation in Urban Environment: A Review". Renewable and Sustainable Energy Reviews, vol. 37, 2014.
[9] A. Rezaeiha, I. Kalkman and B. Blocken, "CFD simulation of a vertical axis wind turbine operating at a moderate tip speed ratio: Guidelines for minimum domain size and azimuthal increment". Renewable Energy, vol. 107, pp. 373–385, 2017.
[10] A. Rezaeiha, H. Montazeri and B. Blocken, "Towards accurate CFD simulations of vertical axis wind turbines at different tip speed ratios and solidities: Guidelines for azimuthal increment, domain size and convergence". Energy Conversion and Management, pp. 301–316, 2018.
[11] P. F. S. Trentin, P. H. B. B. Martinez, G. B. Santos, E. E. Gasparin and L. O. Salviano, "Screening analysis and unconstrained optimization of a small-scale vertical axis wind turbine". Energy, vol. 240, 2022.
[12] P. H. M. Barros and L. O. Salviano, "Sensitivity analysis of a Small-Scale Darrieus vertical axis wind turbine". Proceedings of the XLI Ibero-Latin-American Congress on Computational Methods in Engineering, ABMEC, Foz do Iguaçu/PR, Brazil, November 16-19, 2020.
[13] I. Hashem and M. H. Mohamed, "Aerodynamic performance enhancements of H-rotor Darrieus wind turbine". Energy, 2018.
[14] C. J. Bai, Y. Y. Lin, S. Y. Lin and W. C. Wang, "Computational fluid dynamics analysis of the vertical axis wind turbine blade with tubercle leading edge". Journal of Renewable and Sustainable Energy, vol. 7, 2015.
[15] I. B. Celik *et. al.*, "Procedure for estimation and reporting of uncertainty due to discretization in CFD applications". Journal of Fluids Engineering, Transactions of the ASME, vol. 130, 2008.
[16] A. Tummala *et. al.*, "A review on small scale wind turbines". Renewable and Sustainable Energy Reviews, vol. 56, 2016.
[17] F. Balduzzi *et. al.*, "Critical issues in the CFD simulation of Darrieus wind turbines". Renewable Energy, vol. 85, 2016.
[18] M. R. Castelli, A. Englaro and E. Benini, "The Darrieus wind turbine: Proposal for a new performance model prediction model based on CFD". Energy, vol. 36, pp. 4919–4934, 2011.
[19] Q. Li, T. Maeda, Y. Kamada, J. Murata and K. Furukawa, "Effect of number of blades on aerodynamic forces on a straight-bladed Vertical Axis Wind Turbine". Energy, 2015.
[20] N. E. Helwig and P. Ma, "Smoothing spline ANOVA for super-large samples: Scalable computation via rounding parameters". Statistics and its interface, vol. 9, 2016.
[21] C. Gu. Smoothing Spline ANOVA Models (Second ed.). New York: Springer-Verlag, 2013.
[22] K. Li, "Asymptotic Optimality for C_p, C_L, Cross-Validation and Generalized Cross-Validation: Discrete Index Set". The Annals of Statistics, vol. 15, pp. 958–975, 1987.
[23] G. Wahba. Spline models for observational data. Philadelphia: Society for Industrial and Applied Mathematics, 1990.
[24] L. Ricco and A. Turco, "Smoothing spline ANOVA for variable screening". Dolomites research Notes on Approximation, vol. 6, 2013.
[25] Q. Wang et al, "Statistical Design of Experiment (DoE) based development and optimization of DB213 in situ thermosensitive gel for intranasal delivery". International Journal of Pharmaceutics, vol. 539, pp. 50–57, 2018.